January 2022

A Development Of A General Heat Transfer Correlation For Boiling Two-Phase Flow Of Pure Ethanol Based On Experimental Datasets And Correlations

Mohamed Elfaham

A Development of a General Heat Transfer Correlation for Boiling Two-Phase Flow of Pure Ethanol Based on Experimental Datasets and Correlations.

by

Mohamed ElFaham

Bachelor of Science in Mechanical Engineering, Arab Academy for Science and Technology, 2017

A Thesis
Submitted to the Graduate Faculty

Of the

University of North Dakota

in partial fulfillment of the requirements

for the degree of
Master of Science

Grand Forks, North Dakota
August 2022

This thesis submitted by Mohamed ElFaham in partial fulfillment of the requirements for the Degree of Master of Science from the University of North Dakota, has been read by the Faculty Advisory Committee under whom the work has been done and hereby approved.

Clement Tang

Date

Dr. Surojit Gupta

Date

Dr. Anjali Sandip

Date

This thesis is being submitted by the appointed advisory committee as having met all the requirements of the School of Graduate Studies at the University of North Dakota and is hereby approved.

Chris Nelson
Dean of the School of Graduate Studies

Date

PERMISSION

Title	A Development of a General Heat Transfer Correlation for Boiling Two-Phase Flow of Pure Ethanol Based on Experimental Datasets and Correlations
Department	Mechanical Engineering
Degree	Master of Science

In presenting this thesis in partial fulfillment of the requirements for a graduate degree from the University of North Dakota, I agree that the library of the University shall makeit freely available for inspection. I further agree that the permission for extensive copying for scholarly purposes may be granted by the professor who supervised my thesis work or, in his absence, by the Chairperson of the department or the dean of the School of Graduate Studies. It is understood that any copying or publication or other use of this thesis or part thereof for financial gain shall not be allowed without my written permission. It is also understood that due recognition shall be given to me and to the University of North Dakota in any scholarly use which may be made of any material in my thesis.

Mohamed ElFaham

May 2022

Table of Contents

LIST OF FIGURES

LIST OF TABLES

ACKNOWLEDGEMENT

I would like to express my deep and sincere gratitude to my research supervisor Dr. Clement Tang for giving me the opportunity to do this research and providing invaluable guidance throughout this journey. This endeavor would not have been possible without his guidance, patience, motivation and immense knowledge.

Besides my advisor, I'm extremely grateful to my committee members Dr. Surojit Gupta and Dr. Anjali Sandip for their encouragement, insightful comments and incredible support.

Moreover, I would like to express my deepest appreciation to my friends and colleagues who helped me throughout this journey. I would be remiss in not mentioning Dr. Tarek Elderini for providing me all kind of support, guidance and honest advises.

Finally, Words cannot express my gratitude to my family for their love, prayers, caring and sacrifices. I would like to extend my sincere thanks to my uncle and my best friend Dr. Essam ElFaham for everything he has done, I could not have undertaken this journey without him.

ABSTRACT

Two-phase flow heat transfer has gained an extensive focus over the past decades in many industrial applications and thermal systems. Flow involving phase change due to boiling or condensation exhibits much higher heat transfer coefficient compared to single-phase flow when it is only sensible heat transfer involved. The knowledge of heat transfer coefficients and their parametric behaviors can be utilized to improve the accuracy of models used for designing and optimizing heat transfer equipment for more effective thermal management applications.

In two-phase flow boiling heat transfer, the working fluid can a single pure fluid or a binary fluid mixture. In present study, a systematic methodology is used to compare the available correlations and experimental data in the literature for pure ethanol and ethanol/water binary mixtures at various physical properties. When evaluating the experimental data available in the literature, the availability of data for flow boiling of ethanol, both as pure fluid or binary mixtures, is found to be limited.

The current data that this study has collected for flow boiling of ethanol covers the ranges for mass flux of 0.33 to 290 kg/m2·s−1, heat flux of 2.8 to 40 kW/m2, operating gage pressure of 18 to 135 kPa, and saturation temperature of 40 to 86°C. The correlations that have high accuracies in predicting the experimental data available in the literature are identified and discussed.

CHAPTER 1
Introduction

1.1 Motivation and Problem Statement

The importance of accurately predicting flow boiling heat transfer coefficients has been well recognized, as a large number of analytical and experimental investigations have been conducted by many researchers.

A knowledge of these coefficients and their parametric behavior can help improve the accuracies of models used for designing and optimizing heat transfer equipment, such as evaporator and condenser.

The main focus in this study is to compare boiling two-phase flow heat transfer coefficient of pure ethanol for the available experimental datasets with the theoretical datasets generated by different flow boiling correlations.

Moreover, this process will facilitate the selection process of the correlation with lowest error band and therefore making the needed development to derive a general correlation to calculate two-phase flow boiling heat transfer for the pure component of ethanol. This investigation will be very valuable due to the huge shortage of theoretical and experimental data set of pure ethanol.

1.2 Procedure and Methodology

In order to develop a general correlation, it is essential to have an extensive database covering different fluids with a wide range of operating conditions such as mass flux, heat flux, pressure, vapor quality, and tube diameter. Moreover, the flow

patterns (e.g., annular flow, bubbly flow, etc.) and the tube orientation (e.g. vertical, horizontal, etc.) are considered as factors influencing heat transfer coefficient. There are a various number of heat transfer correlations for boiling flow which can be tested and used for comparison with experimental dataset.

1.3 Scope of Work

A 720 data point has been collected from various experimental work that exist in literature. This data points have different parameters based on the experimental procedure made by the authors. The range of parameters that has been used in all the experiments are shown in Table 1.

Table 1 Experimental conditions used in pure ethanol dataset

Parameters	**Range**
Saturation Temperature T_{sat}	40 – 86.6
Mass Flux G (kg/m^2 s)	0.33 – 290
Heat Flux q Kw/m^2	2.8 - 104
Internal Diameter d_{in}	5 - 10
Vapor Quality x	0.11 – 0.91

These parameter has been used to generate the thermophysical properties of pure ethanol (e.g. densities, thermal conductivity, specific heat, viscosity ... etc.) for the liquid phase and vapor phase. Therefore, generating theoretical dataset using 14 correlations exist in literature and will be discussed in chapter 4.

At this point, by having an experimental dataset and theoretical dataset, this will initiate the comparison process. The major point of comparison is the mean

absolute error, which shows the most precise correlation in the 14 correlations that have been used.

Therefore, selection of the best correlation with lowest error band will be significant in developing a more precise general correlation for predicting the two-phase flow heat transfer coefficient of the pure component of ethanol.

CHAPTER 2
Boiling Heat Transfer

Boiling heat transfer is defined as a type of heat transfer that occurs with a phase change from liquid to vapor. There are two fundamental types of boiling. Flow and pool boiling. Flow boiling is boiling in a flowing stream of fluid, where the heating surface may be the channel wall confining the flow. A boiling flow is composed of a mixture of liquid and vapor and is the type of two-phase flow which is the flow of a medium consisting of two phases (e.g., gas (vapor) and liquid, gas (vapor) and solid, liquid and solid) [1].

While pool boiling is boiling on a heating surface submerged in a pool of initially quiescent liquid. Due to the very high heat transfer rate in boiling, it has been used to cool devices requiring high heat transfer rates, such as rocket motors and nuclear reactors. Its applications in modern industry are so important that large amounts of research in many countries have been devoted to understanding its mechanisms and behavior [1].

2.1 Boiling Regimes

There are several boiling regimes in pool boiling as well as in flow boiling. The only difference lies in the influence of flow effect. The buoyancy effect is significant in a pool boiling system, while the flow forced-convection effect is significant in flow boiling inside a channel. These boiling regimes were observed by previous researchers, namely, Leidenfrost (1756), Lang (1888), McAdams et al. (1941), Nukiyama (1934), and Farber and Scorah (1948) [1].

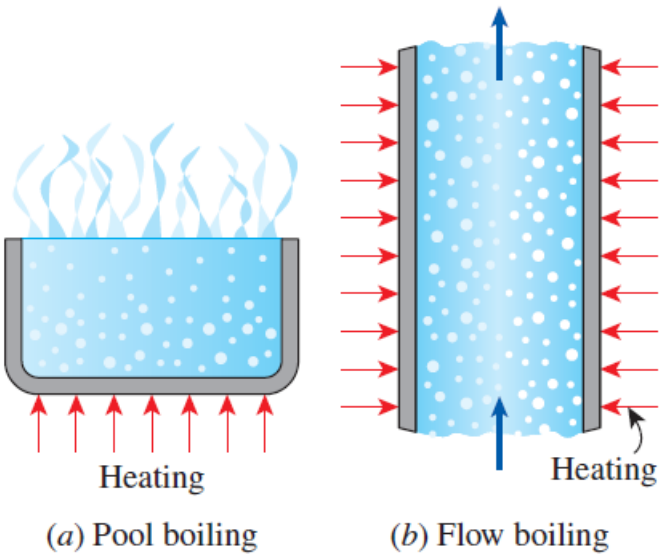

Figure 1 Difference between Pool and flow boiling[2]

2.2 Two Phase Pool Boiling

Generally, it means the boiling of fluids in stationary position, the fluid is not imposed to flow by an external source. Thus, any motion of fluid is because of the natural convection. The fact is Pool boiling refers to vaporization that takes place at a solid surface submerged in a quiescent liquid. When the saturation temperature T_s, of the solid surface exceeds the saturation temperature, T_{sat} of the liquid. Vapor bubbles form at nucleation sites on the surface, grow and subsequently detach from the surface. The driving force for heat transfer is $\Delta T_e = T_w - T_{sat}$, called the excess temperature. Liquid circulation in pool boiling occurs by natural convection and by the agitation resulting from bubble growth and detachment. The boiling curve is a plot of surface heat flux versus excess temperature, and has the general features illustrated in Figure 2 which show the following boiling regimes[3].

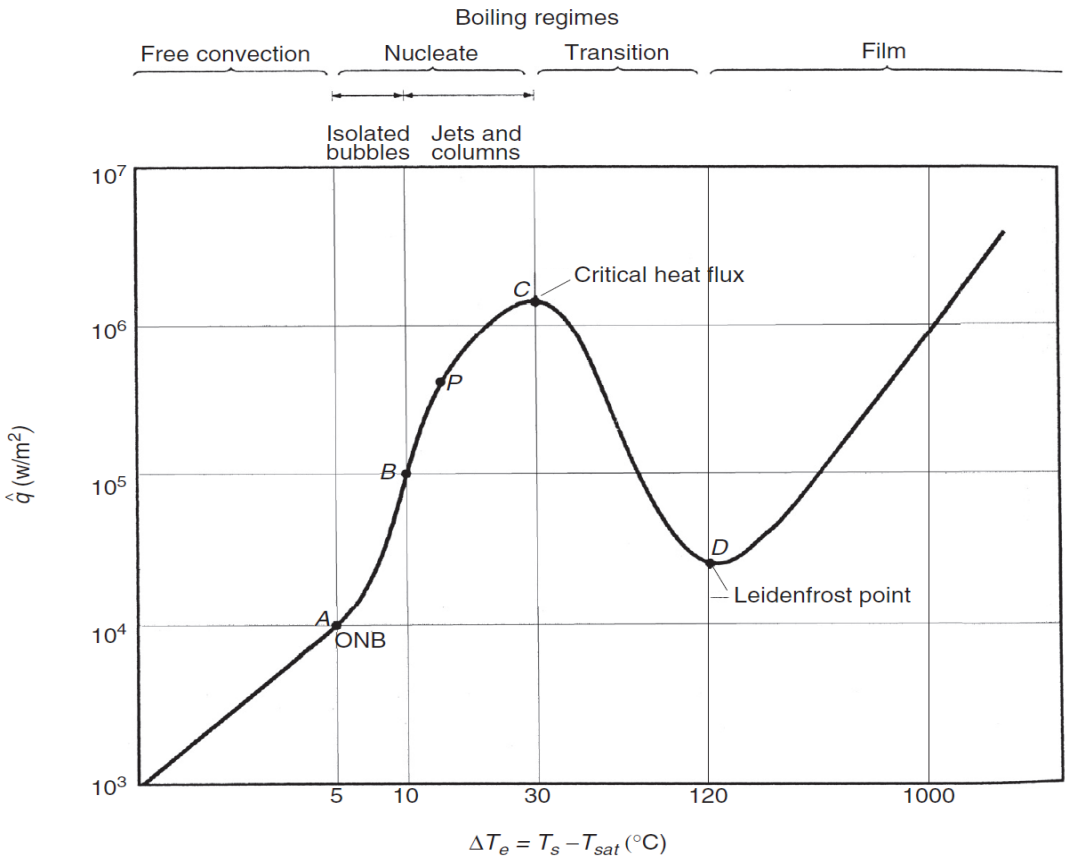

Figure 2 Pool boiling curve for water at 1 atmospheric pressure[3]

Natural Convection Boiling: This phenomena happens when liquid is heated over the saturation temperature. Hence, the liquid is somehow superheated in this instance and evaporates when it rises to the free surface. The heat transfer by the influence of a heating surface to the fluid is caused by natural convection. This occurs as shown in Figure 3(a) when $\Delta T_e < 5$ °C. Point A on the curve marks the onset of nucleate boiling (ONB). At lower excess temperatures, heat transfer occurs by natural convection alone.

Nucleate boiling [A-C]: It exists between points A and C on the curve. Two different boiling regimes can be distinguished in this region. Between points A and B, the boiling is characterized by the formation of isolated vapor bubbles at nucleation

sites dispersed on the solid surface. Bubble growth and detachment result in significant fluid mixing near the solid surface that greatly increases the rate of heat transfer. In this regime, heat is transferred primarily from the solid surface directly to the liquid flowing across the surface. As the heat flux increases beyond point B, the number of active nucleation sites and the rate of vapor formation become so great that bubble interference and coalescence occur.

The vapor leaves the solid surface in jets or columns that subsequently merge and form large slugs of vapor. The high rate of vapor formation begins to inhibit the flow of liquid across the solid surface, causing the slope of the boiling curve to decrease. An inflection point occurs at point P; here, the heat-transfer coefficient reaches a maximum.

The heat flux continues to increase between points P and C since the increase in temperature driving force more than compensates for the decreasing heat-transfer coefficient. The heat flux attains a maximum, called the critical heat flux, at point C. This occurs as shown in Figure 3(b) when $5\ ^\circ C < \Delta T_e < 30\ ^\circ C$

Transition boiling [C-D]: At this region, the rate of vapor formation is so great that some parts of the surface are covered by a continuous vapor film. Since heat-transfer rates for gases are generally much lower than for liquids, the overall rate of heat transfer begins to decrease.

Although the vapor film tends to be unstable, breaking up and reforming at any given point, the fraction of the solid surface covered by vapor continues to increase

from point C to point D. This region, in which the heat flux decreases as ΔTe increases. This occurs as shown Figure 3 (c) when 30 °C < ΔT_e < 200 °C.

Film boiling: The heat flux reaches a minimum at point D, the so-called Leidenfrost point, where the entire solid surface is covered by a vapor blanket. Beyond this point, heat is transferred from the solid surface across the vapor film to the liquid. Hence, this regime is called film boiling. As indicated in Figure 1, very high surface temperatures may be reached in film boiling, and consequently radiative heat transfer can be significant in this regime. This occurs as shown in Figure 3 (d) ΔT_e > 200 °C.

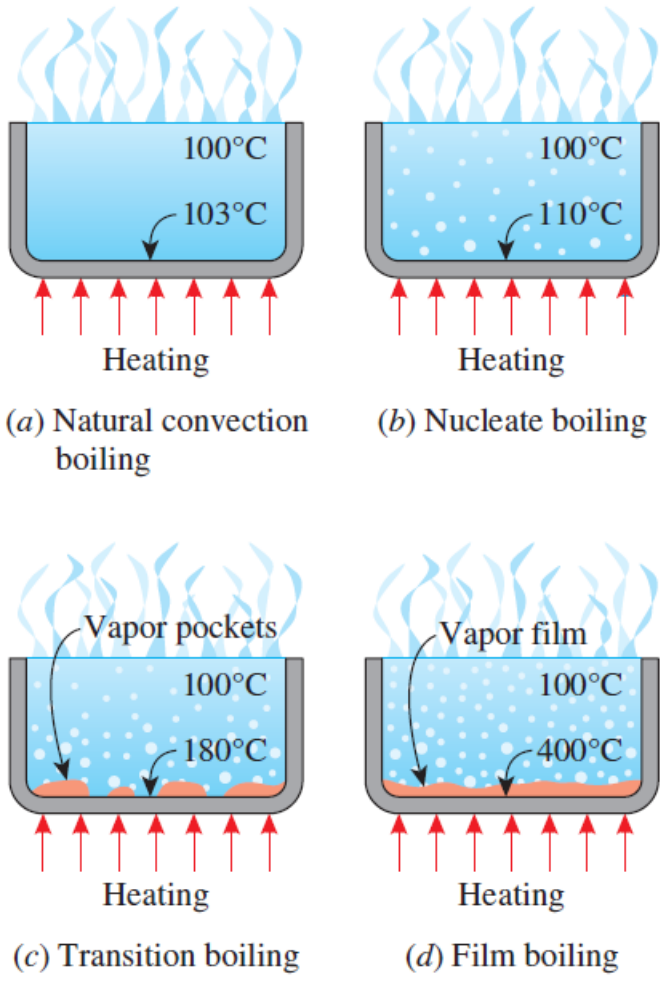

Figure 3 The effect of ΔT_e on different boiling regimes in Pool boiling[2]

Most reboilers and vaporizers are designed to operate in the nucleate boiling regime. Although film boiling is sometimes employed, the much higher temperature driving force (corresponding to a much lower heat-transfer coefficient) in this regime generally makes it unattractive compared with nucleate boiling. The transition region, with its unusual characteristic of decreasing heat flux with increasing driving force, is always avoided in equipment design[1, 3].

CHAPTER 3
Two-Phase Flow Boiling Heat Transfer

Two phase or Gas–liquid flows occur widely in both nature and industrial applications, including energy production (e.g., oil transportation, steam generators, cooling systems) and chemical engineering (e.g., bubble columns, reactors, aeration systems). Two-phase flow in micro-channels have attracted attention because of its wide applicability to such advanced fields as electronic cooling, medical and genetic engineering, bioengineering, etc.

There are a variety of fluids can be used in such a system (water, helium, nitrogen, R-11, R-22, hydrocarbons, etc.) but due to the significant growing of the world population and energy consumption, some restrictions as have been made for working fluid selection to avoid any environments problems such as: Ozone depletion, global warming, acid rains, air pollution, …etc.

3.1 Pure Ethanol in Two-Phase Flow

Pure ethanol is considered to be a very promising fluid as it shows an intermediate thermodynamic and transport characteristic as shown in the T-S diagram in figure 4 [4]. However, there is a large shortage of experimental data for pure ethanol in literature.

Most of the available experimental data that exists in literature has been collected to be analyzed in the research. It will be discussed in detail in the results and discussion section. Pure ethanol requires a lower amount of heat for establishing of boiling, due to its thermophysical properties.

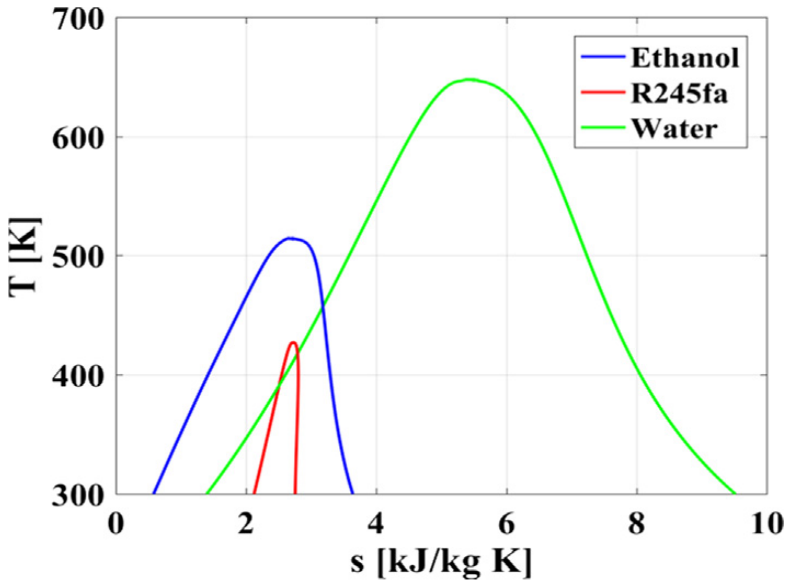

Figure 4 T-s diagram for ethanol, refrigerant R245fa and water[4]

Mastrullo et al. [4] studied experimentally anhydrous ethanol (purity grade of 99.8%). All the flow boiling tests have been performed in the same horizontal SS316 stainless steel tube of 6.0 mm, by using different operating parameters in terms of mass flux, saturation temperature and heat flux. Particularly, mass velocities from 85 to 127 kg/m2 s have been investigated, whereas the saturation temperature has been fixed from 64.5 up to 85.8 °C. And the imposed heat flux from 10.0 up to 40.3 kW/ m^2.

According to the authors, it was found that the local heat transfer efficient show a pure convective behavior, having an increasing trend with vapor quality up to the occurrence of dry-out. Pure ethanol has been tested for heat pipe applications with positive outcomes. Furthermore, Robertson et al. [5] experimentally investigated the vertical boiling of ethanol in 10 mm tube inside diameter , 3 m long was used in the experiment. They used a wide range of heat fluxes, vapor quality with range 0.03 ~ 0.6 and two mass velocities (145, 290 Kg/m^2. S).

The authors show the interaction between nucleate and convective boiling as a function of vapor quality, based on precise measurements of ethanol at saturation conditions. Moreover, Vasileiadou et al.[6] investigated the two-phase flow heat transfer for pure ethanol in borosilicate glass based with tantalum surface vertical square channel with 5 mm inner hydraulic diameter, wall thickness 0.7 mm, heated length 72 mm , heat flux with range 2.8–6.1 kW/m^2 , Mass flux : 0.33–1.0 kg/m^2 . S and Saturation Temperature: 40 °C.

The authors show the effect of fluid composition in the flow boiling heat transfer by the addition of ethanol into water (5%v/v) could enhance the heat transfer coefficient in comparison to the pure components. Also, they concluded that the amplitude of wall temperature heating fluctuation is absolutely lower than for pure liquids, allowing for a more stable heat transfer process. In addition, Peyghambarzadeh et al. [7] experimentally studied the effect of the working fluid among water, ethanol, and methanol on the thermal performance of a 40 cm circular copper heat pipe.

Heat flux with range up to 2500 W/m^2 were applied to the evaporator along with a constant water temperature was used at three levels including 15, 25, and 35 °C in the condenser. The authors stated that heat transfer coefficient for ethanol and water were higher than methanol and it was also noticed that increasing the heat flux causes an increase of the heat transfer coefficient of the evaporator.

Moreover, the usage of ethanol led to higher heat transfer coefficient. As well as, Diaz and Schmidt [8] presented an experimental investigation of flow boiling heat transfer of pure water and ethanol in a single 0.3×12.7 mm^2 rectangular mini channel made up of nickel alloy Inconel 600 and electrically heated. The authors explored mass

fluxes between 50 and 500 kg/m^2 s and heat fluxes up to 400 kW/m^2, at atmospheric pressure. They found that, after the low vapor quality region, the heat transfer coefficient increased with increasing vapor quality only in case of a low imposed heat flux. The trend was found to be instead reversed with increasing heat flux.

3.2 Boiling regimes

Two -phase flow is substantial in heat transfer and process systems including reboilers, heat exchangers, highly powered electronic systems cooling, catalytic reactor and refrigeration systems [9]. It shows a huge Functionality to improve the accuracy of models used for designing and optimizing heat transfer equipment for more effective thermal management applications. Two-phase evaporative flow is more attractive due to the utilization of latent heat and the higher heat-transfer coefficient achieved compared to single phase flow. It revealed a high heat flux dissipation and compactness[10].

Besides an active policy of energy saving for all the residential and industrial activities, there is an increasing force in the research of sustainable and economically feasible technologies for efficient and clean overtures to the energy conversion and utilization**.**

At present, the knowledge of flow and heat transfer in micro-scale flow passages of a size less than 100 μm is thus strongly demanded. Specifically, fundamental knowledge of two-phase flow characteristics in small flow passages, such as the pressure drop, heat transfer coefficient, flow pattern, and void fraction , is crucial for engineering design purposes as well as for evaluation of practical performance.

However, our current knowledge is still limited and in reality, only a small number of literature sources are available. One of the questions is whether the two-phase flow patterns in small size channels are different from those encountered in ordinary size channels.

In particular, the large tubes and the tubes of a small range of millimeters in diameter, the patterns of the two-phase flow are affected mostly by gravity with minimal surface tension effects. On the other hand, in micro-channels with the diameter on the order of a few microns to a few hundred microns, two-phase flow is believed to be influenced mainly by surface tension, viscosity and inertia forces. Entrance and surface roughness effects. There is an important resemblance between two-phase flow in microchannels and the flow in large channels at micro-gravity.

In both system types the inertia, viscosity, and surface tension are major parameters, while buoyancy is suppressed. Consequently, two-phase dimensionless parameters that have previously been developed for micro-gravity might be useful for micro-channels.

3.3 Two-Phase Flow regimes

When a vapor-liquid mixture flows through a circular tube, a number of different flow regimes can occur, depending on the vapor fraction, flow rate, and orientation of the tube. Nevertheless, flow patterns or flow regimes these can be categorized into forms of interfacial distribution. Comprehensive discussions of these patterns are disscused by Hewitt [11], Whalley[12] and Dukler and Taitel [13].

3.4 Two-phase flow regimes for vertical tubes

When a vapor-liquid mixture flows through a circular tube, a number of different flow regimes can occur, depending on the vapor fraction, flow rate, and orientation of the tube. For vertical tubes, the following flow regimes are distinguished (Figure 5):

- **Bubble flow:** At low vapor fractions, vapor bubbles are dispersed in a continuous liquid phase.
- **Slug/Plug flow:** At moderate vapor fractions and relatively low flow rates, large bullet-shaped vapor bubbles flow through the tube separated by slugs of liquid in which smaller bubbles may be dispersed. where the bubbles have merged to make bigger bubbles in which be similar to the diameter of the tube.
- **Churn- flow:** At higher flow rates, the large vapor bubbles present in slug flow become unstable and break apart, resulting in an oscillatory, or churning, motion of the liquid upward and downward in the tube.
- **Annular flow:** At high vapor fractions and high flow rates, the liquid flows as a film along the tube wall while the vapor flows at a higher velocity in the central region of the tube. Small liquid droplets are usually entrained in the vapor phase, and vapor bubbles may be dispersed in the liquid film as well.

At sufficiently high liquid flow rates, the droplets coalesce to form large streaks or wisps of liquid entrained in the vapor phase. This condition, which is characteristic of flows with a high mass flux, is referred to as **wispy annular flow**.

- **Mist Flow:** At very high vapor fractions, the liquid phase exists entirely as droplets entrained in a continuous vapor phase.

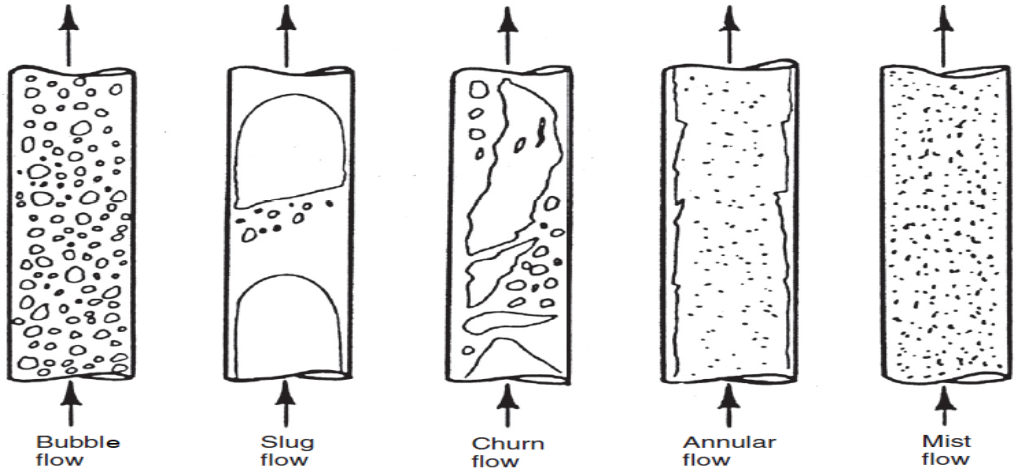

Figure 5 Flow patterns in vertical flow[3]

3.5 Two-phase flow pattern transitions in vertical flow

Bubble-Plug transition: This transition traditionally has been occurred as a result of bubble overlapping causing a gradual bubble growth. Mainly, the process of transition to slug flow happens when the void fraction is around 0.25~0.3. Usually, break-up of the bubbles may be assumed to happen in highly turbulent flows to offset the progression of the coalescence. Furthermore, the recent information seems to show that this view of the transition may be incorrect. It looks like that the formation of void

waves in the flow in which the bubbles turn into a compact and are more able to merge leading to plug flow [14].

Plug-annular flow transition: This area is a major argument. churn flow which is very important ain development of plug or slug flow[13]. As long as, churn flow which is characterized here will occur in fully developed flow, and has the following characteristics:

- The regime takes place from slug flow by the establishment of flooding-type, and these continue as a main characteristic of the regime all through. These waves does not exist in both slug and annular flow but are formed repetitively in the churn flow regime and transport it upwards [15].
- In between consecutive flooding waves, the liquid phase flow in the film region close to the wall keeps direction and is eventually dragged by the next upward-moving wave.

Churn to annular flow transition: By increasing the gas velocity after entering the churn flow, the pressure gradient decreases until reaching a minimum value. The flooding waves and their accompanied intensive gas-liquid interactions generate large pressure gradients and as they disappear, the pressure gradient decreases.

3.6 Two-Phase Flow regimes for horizontal tubes

In horizontal tubes the situation is somewhat different due to stratification of the flow resulting from the gravitational force. The following flow regimes are observed in Figure 6:

- **Bubbly flow:** The flow pattern is similar to that in vertical tubes except the bubbles tend to concentrate in the upper part of the tube.
- **Plug flow:** The flow pattern is similar to slug flow in vertical tubes, but the bullet-shaped bubbles tend to flow closer to the top of the tube and occupy less of the tube cross-section.
- **Stratified flow:** The two phases are completely stratified, with the liquid flowing along the bottom of the tube and the vapor flowing along the top.
- **Wavy flow:** In stratified flow at higher vapor velocities, waves are formed on the surface of the liquid that characterize this flow regime.
- **Slug flow:** In this regime, intermittent slugs of liquid pass through the tube. The slugs occupy the entire tube cross-section and contain a large number of entrained vapor bubbles that impart a frothy character to the liquid.
- **Annular flow:** The flow pattern is similar to annular flow in vertical tubes except that the liquid film thickness is non-uniform, being greater on the bottom than the top of the tube.
- **Mist flow:** The flow pattern is the same as in a vertical tube and, hence, is not illustrated for the horizontal tube in Figure. 6, Flow pattern maps, which show the operating regions over which the various flow regimes exist.

The latter also discusses modeling and empirical correlations for predicting the frictional pressure drop in each flow regime. However, most process equipment design

is based on generalized pressure drop correlations that do not explicitly account for the two-phase flow regime. These correlations are presented in the following subsection.

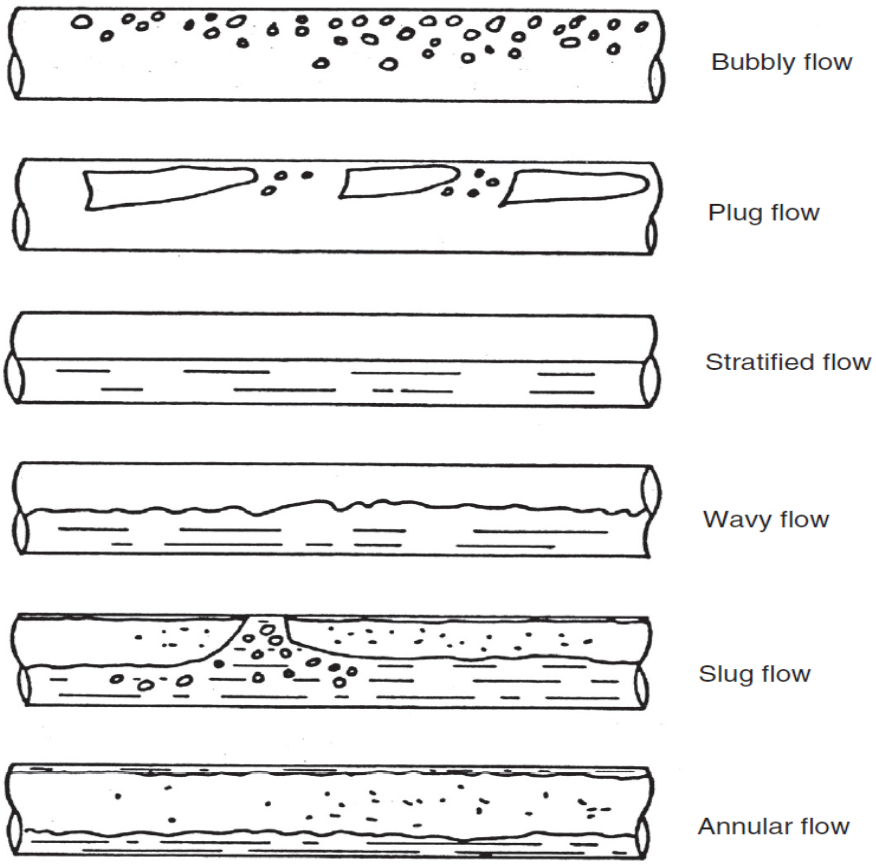

Figure 6 Flow Patterns in horizontal flow[3]

3.7 Comparison between Pool and flow boiling

Flow boiling has more advantage rather than pool boiling in heat transfer performance, due to its convective cooling nature and has been widely and irreplaceably used in fields related to high power densities. The combination of liquid/gas mixture either in pure component or binary mixture has proven a significant enhancement in heat transfer coefficient due to the bubble formation. Therefore, the

study of pure components and their effect on heat transfer coefficient are widely investigated in literature. Moreover, predicting critical heat flux in boiling heat transfer is very important, as it is the critical point between nucleate boiling and film boiling regimes as shown in the curves of flow and pool boiling in Figure 7. The existence of critical heat flux is usually associated with an excessive increase in the surface temperature for a surface heat flux controlled system, while an significant reduction of the heat transfer rate appears to the surface temperature controlled system.

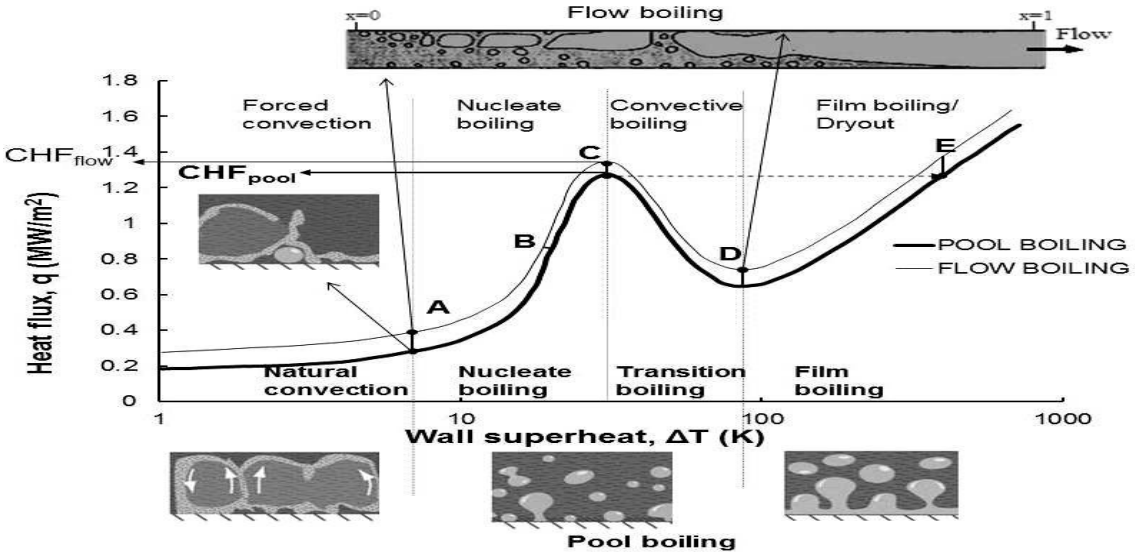

Figure 7 Pool and flow boiling water curve by Nukiyama 1984 [16]

It is known that the presence of dry spots on heated surfaces at high heat fluxes is a typical characteristic of nucleate boiling for a surface heat flux-controlled system. The major effects that have been studied towards pool and flow boiling of pure fluids and binary/multicomponent mixtures are summarized, as shown in Fig. 8. Where also the key difference between pool boiling and flow boiling is that pool boiling occurs in the absence of bulk fluid flow, whereas flow boiling occurs in the presence of bulk fluid flow. Pool boiling further classified natural and forced boiling. While flow boiling further classified in adiabatic and diabatic boiling.

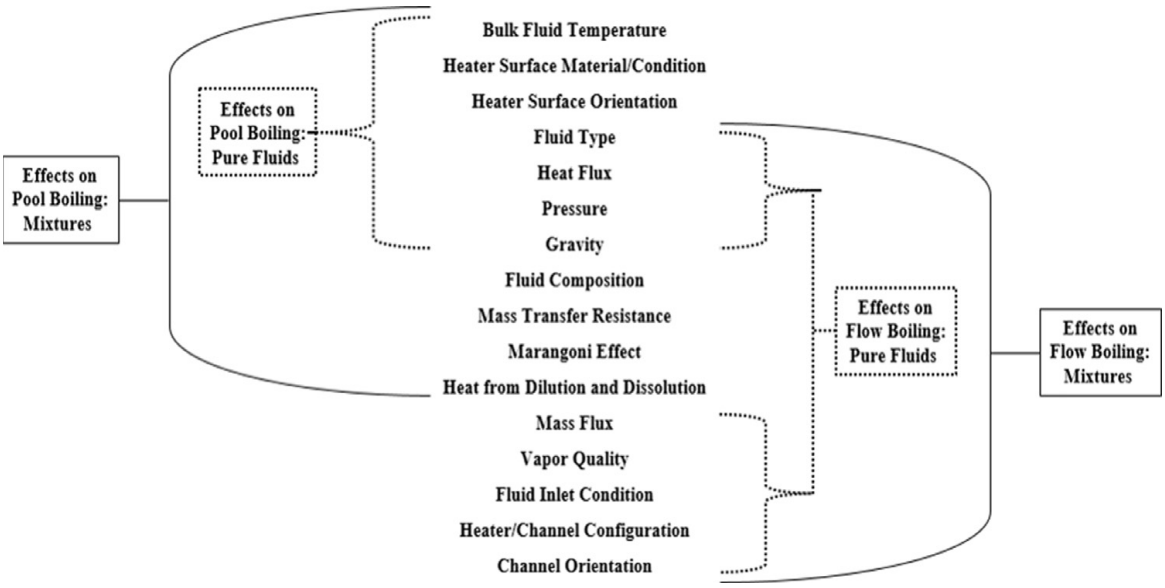

Figure 8 Summary of major effects on pool and flow boiling of either pure fluids or binary/multicomponent mixtures [17]

CHAPTER 4
Heat Transfer Coefficient Correlations

The importance of accurately predicting flow boiling heat transfer coefficients has been well recognized, as a large number of analytical and experimental investigations have been conducted by many researchers. A knowledge of these coefficients and their parametric behavior can help improve the accuracies of models used for designing and optimizing heat transfer equipment, such as evaporator and condenser. Each correlation has its own range of data, specific experimental geometry, type of channels (e.g., Macro, Mini channels) and type of fluid used in its development, in which going beyond it will not be highly reliable. Therefore, the data from various sources which could not be satisfactorily correlated by existing correlations were shown to be quite well correlated by their own data and the fluids that have been used in deriving their own correlations.

4.1 Chen Correlation

One of the leading correlation methodologies used to calculate the heat transfer coefficient in convective boiling has been proposed by Chen [18]. Such correlation was established from 10 experimental scenarios using more than 600 data points including various liquids such as methanol, water, cyclohexane, benzene, heptane, and pentane in vertical tubes. Moreover, he declared the ranges for vapor quality, pressure and mass flux to be 0.1 ~ 0.71, 8 ~ 14 psia, and 6.2 ~ 240 kW/m^2. S, respectively.

His experimental work was based on a superposition model assumption such that the nucleate pool boiling was added to the convective heat transfer coefficient.

Nevertheless, a result of convection is the suppression of nucleate boiling. According to Chen, the reduction in the difference of temperature between the inner wall of the tube and the bubbles mounting outside it takes place due to the temperature gradient drop near the tube wall along with the increase in the flow rate. Hence, he proposed the ratio between the effective temperature difference between overall temperature difference and the bubble growth, named as Chen Suppression Factor (S_{CH}). Furthermore, he has also represented the convective heat-transfer coefficient in terms of only the liquid phase heat transfer coefficient, h_L [19, 20], given by Eq.1.

$$h_{fc} = F(X_{tt}).h_L \qquad \textit{(Eq. 1)}$$

Chen has used the values of S_{CH} and $F(X_{tt})$ in the experimental database graphically. These values have been replaced by curve-fit equations to obtain the following form of the Chen correlation.

$$h_{TP} = S_{ch}\,.h_{nb} + F(X_{tt}).h_L \qquad \textit{(Eq. 2)}$$

Where:

$$S_{ch} = (1 + 2.53 \times 10^6\, Re^{1.17})^{-1} \qquad \textit{(Eq. 3)}$$

$$h_{nb} = \frac{K_L^{0.79}.C_{p_L}^{0.45}.\rho_L^{0.49}.\Delta T_e^{0.24}.\Delta P_{sat}^{0.75}}{\sigma^{0.5}.\mu_L^{0.29}.\,\Delta h_{vp}^{0.24}\,\rho_V^{0.24}} \qquad \textit{(Eq. 4)}$$

$$F(X_{tt}) = 2.35(X_{tt}{}^{-1} + 0.213)^{0.736} \qquad (X_{tt} < 10) \qquad \textit{(Eq. 5)}$$

$$F(X_{tt}) = 1 \qquad (X_{tt} \geq 10) \qquad \textit{(Eq. 6)}$$

$$h_L = 0.023\,.\left(\frac{K_L}{D_L}\right).Re_L^{0.8}.Pr_L^{0.4} \qquad \textit{(Eq. 7)}$$

$$Re_L = \frac{D_i.G_L}{\mu_L} \qquad \textit{(Eq. 8)}$$

Reynolds number mentioned in the previous equation (eq.8) was calculated using the mass flow rate of the liquid phase only. Chen calculated the has nucleate

boiling heat-transfer coefficient (h_{nb}) by using the Forster–Zuber correlation [21] and therefore for estimating a conservative for mixtures. It has also extensively been employed for many years and is still the standard of comparison for new correlations.

4.2 The Gungor–Winterton correlation

The correlation of Gungor and Winterton [22] is similar in form to the Chen correlation [18] in that the nucleate boiling and convection terms are additive. Due to the effect of convective boiling heat transfer, a suppression factor S_{GW} and convective enhancement factor E_{GW} were included. h_{sp} is calculated using the Cooper correlation [23] , and the Dittus–Boelter (Eq.7) is used for the forced convection coefficient. Based on 4800 data points from 28 source using the following fluids: Water, ethylene glycol, R11, R12, R22, R113, R114. The authors stated the following parameters regarding pressure and diameter are 2.95 ~ 32 mm and 0.08 ~ 202.6 bar respectively.

The correlation gives HTC values that slightly decrease with increasing vapor quality.

$$h_{TP} = S_{GW} \cdot h_{nb} + E_{GW} \cdot h_L \qquad \textit{(Eq. 9)}$$

$$S_{GW} = (1 + 1.15 \times 10^{-6} \cdot E_{GW} \cdot Re_L^{1.17})^{-1} \qquad \textit{(Eq. 10)}$$

$$E_{GW} = 1 + 24{,}000 \cdot B_o^{1.16} + 1.37 \cdot X_{tt}^{-0.86} \qquad \textit{(Eq. 11)}$$

$$B_o = \frac{q}{\Delta h_{vp} \cdot G} \qquad \textit{(Eq. 12)}$$

Gungor-Winterton has used cooper correlation for calculating the nucleate boiling heat transfer value instead of using Forster-Zuber correlation [21] as proposed in Chen correlation [18] as shown in the following equation:

$$h_{nb} = 55 \cdot q^{0.67} \cdot P_r^{0.12} \cdot (-log_{10} P_r)^{-0.55} \cdot M^{-0.5} \qquad \textit{(Eq. 13)}$$

Where P_r and M are the reduced pressure and molecular weight. Due to the boiling number term in enhancement factor equation, it does not reduce to unity when the vapor fraction is zero. Moreover, the correlation provides a pretty good representation of the data, especially for refrigerants in the saturated boiling regime.

The constants S_{GW} and E_{GW} were determined by a complex iterative regression procedure, where the nucleate and convective terms are strongly coupled through derived equation of E_{GW}. Therefore, it is inadvisable to substitute cooper correlation for calculating the nucleate boiling heat transfer coefficient to correlation in the proposed correlation by Gungor and Winterton [22].

4.3 The Liu–Winterton Correlation

Liu and Winterton [24] has used the same data as Gungor-Winterton[22] to develop a flow boiling correlation that based on the method of combining the two contributions suggested by Kutateladze [25] for vertical and horizontal tubes. It provides a significantly better fit to the data than the latter correlation in both the saturated and subcooled boiling regimes.

This correlation values are the closest to those obtained in the experiments, but at low values of quality, h_{tp} usually increases with quality. Furthermore, Reynold's number were calculated in Liu-Winterton correlation[24] as in [Eq.8] using the term G not (1-x). G to calculate the single-phase liquid heat transfer coefficient and the nucleate boiling suppression factor, which considered as a significant difference between their proposed correlation and the others. The correlation developed by Liu and Winterton [24] is described by the following equations:

$$h_{TP} = [(S_{LW} \,.\, h_{nb})^2 \;+\; (E_{LW}.\, h_L)^2]^{\frac{1}{2}} \qquad \textit{(Eq. 14)}$$

$$S_{LW} = (1 + 0.055 \,.\, E_{LW}^{0.1} \,.\, Re_L^{0.16})^{-1} \qquad \textit{(Eq. 15)}$$

$$E_{LW} = [1 + x \,.\, P_{r_L} \frac{(\rho_L - \rho_V)}{\rho_V}]^{0.35} \qquad \textit{(Eq. 16)}$$

For horizontal tubes, the low Froude number corrections are applied to S_{LW} and E_{LW} as in the Gungor–Winterton method[22]. The Cooper[23] and Dittus–Boelter correlations are used to calculate h_{nb} and h_L. Notice that the enhancement factor, E_{LW}, correctly reduces to unity when the vapor fraction, x, is zero. (Eq.14) is a special case of the general formula:

$$h_{tp} = [(a.\, h_{nb})^m + \left(b.\, h_{fc}\right)^m]^{1/m} \qquad \textit{(Eq. 17)}$$

where $1 \leq m < \infty$. Formulas of this type provide a smooth transition between two limiting cases, in this instance between forced convection and nucleate boiling. The abruptness of the transition is governed by the size of the exponent, with larger values of m resulting in more abrupt transitions. This approach has been used to develop many very successful correlations for heat, mass, and momentum transport. This correlation has been used for many decades and still valuable in most of the comparison for new correlations.

4.4 Lazarek and Black Correlation

Lazarek and Black Correlation [26], stated that the strong dependence of heat transfer coefficient on the heat flux with negligible influence of vapor quality shows the dominance of nucleate boiling. It gives a higher h_{tp} value, this correlation was derived based on 728 data points by using R113 as a working fluid. It was stated that

the range of parameters concerning diameter, mass flux, heat flux and pressure were 3.1 mm, 125 ~ 750 Kg/m^2. S , 14 ~ 380 kW/m^2, 1.3 ~ 4.1 bar respectively.

It failed to predict the experimental data in square mini channels with MAE over 80%. This means the correlations developed for macro-channels normally fail to predict data in mini-channels, and vice versa. The correlation was represented by the following equation

$$h_{tp} = 30.Re_L^{0.857}.B_o^{0.714}.\frac{K_L}{d} \qquad \textit{(Eq. 18)}$$

4.5 Kandlikar correlation

Kandlikar [27]added a significant expansion to his collected dataset to be 5246 data points from 24 experimental investigations with ten fluids which are R11, R12, R22 R113, R114, R152a and R13B1,water, neon, nitrogen. Kandlikar proposed a correlation in order to predict the correct HTC for the two phase in terms of vapor quality trend as validated with R-113 and water data. Moreover, an extra testing with the recent R-113 and R-22 data achieved the lowest mean deviations along with the other correlations. The proposed correlation can be expanded to other working fluids by calculating the fluid dependent parameter F_{fl} for that fluid from its pool boiling or flow boiling data. He assumed the addition of the mechanism of nucleate and convective boiling mechanisms for each region.

He started with the vertical-flow data for water. The two-phase flow boiling heat transfer coefficient, h_{tp} was expressed as the sum of the nucleate and the convective boiling terms, given by the following:

$$\frac{h_{TP}}{h_L} = C_1 C_o^{C_2} + C_3 B_o^{C_4} \qquad (Eq.\ 19)$$

where $C_1 C_o^{C_2}$ represents the convective boiling term. On the other hand, $C_3 B_o^{C_4}$ represent the nucleate boiling term. The values of $C_1 \sim C_5$ are represented in Table 2.

Table 2 Constants in proposed correlation

Constant	Convective Region	Nucleate Boiling Region
C_1	1.1360	0.6683
C_2	-0.9	-0.2
C_3	667.2	1058
C_4	0.7	0.7
C_5	0.3	0.3

C_5 =0 for vertical tubes and for horizontal tubes with $Fr_l > 0.04$

The convective and the nucleate boiling regions were also defined based on the convection number (C_O), as shown in the following intervals:

$C_O < 0.65$ "Convective boiling region

$C_O > 0.65$ "Nucleate boiling region"

Concerning the convective boiling region, the heat transfer is primarily by a convective contribution. In addition, the nucleate boiling region, the heat transfer is mostly by nucleate boiling mechanism. Therefore, the effect of heat flux is markedly different in the two regions. The above method of separating the two regions results in a incoherence at *Co* = 0.65. presented in the Shah correlation.

This discontinuity has removed by permitting the transition from one region to another at the intersection of the corresponding correlations. The correlation was then

expanded to other fluids by including a fluid-dependent parameter F_{fl}. Equation (eq.20) is rewritten in a slightly different form, and F_{fl} is included in the second term as follows:

$$\frac{h_{TP}}{h_L} = C_1 C_o^{C_2} + C_3 B_o^{C_4} F_{fl} \qquad (Eq.\ 20)$$

where the value of F_{fl} was diverse over the range from 0.5 ~ 5.0. The value of the fluid dependent parameter showing the lowest mean absolute error for all data sets for that fluid under both convective and nucleate boiling contribution regions was finally chosen. The effect of starting at low flow rates in horizontal tubes was correlated by introducing the Froude number in the nucleate boiling in the convective boiling terms as shown in (Eq.21):

$$\frac{h_{TP}}{h_L} = C_1 C_o^{C_2} (25 F_{r_L})^{C_5} + C_3 B_o^{C_4} \left(25 Fr_L^{C_6}\right) F_{fl} \qquad (Eq.\ 21)$$

Table 3 Fluid dependent parameter F_{fl} in proposed correlation

Fluid	**F_{fl}**
Water	1.00
R-11	1.30
R-12	1.50
R-13B1	1.31
R-22	2.20
R-113	1.30
R-114	1.24
R-152a	1.10
Nitrogen	3.50
Neon	3.50

F_{fl}= 1 for all fluids that flows in stainless steel tubes

The values of constants $C_1 \sim C_5$ are given in Table 2. The constant C_6 in (Eq.21) was found to be zero, and therefore the Froude number multiplier in the nucleate boiling term in (Eq.21,22) is missing. Also, for vertical flow, and for horizontal flow with $F_{r_L} > 0.04$, the Froude number multiplier in the convective boiling term in (Eq.22) becomes unity. The two sets of values given in Table 3 correspond to the convective boiling and nucleate boiling regions, respectively. The heat transfer coefficient at any given condition is evaluated.

Considering the two sets of constants mentioned in Table 3 regarding the two regions along with the transition in between the regions happens at the intersection of the respective correlations. The value of the proposed correlation is determined based on the predicted higher heat transfer coefficient. Since this method delivers a continuity between the nucleate and the convective boiling regions, hence, the final form of the proposed correlation will be as follow:

$$\frac{h_{TP}}{h_L} = C_1\, C_o^{C_2} (25\, F_{r_L})^{C_5} + C_3\, B_o^{C_4}\, F_{fl} \qquad \textit{(Eq. 22)}$$

4.6 Tran et. al correlation

The developed heat transfer correlation[28] is an improvement over the use of either the Cooper or Stephan and Abdelsalam pool boiling correlations to represent nucleate flow boiling in small channels, as both pool boiling correlations underpredict the data over a broad range of wall superheats. The proposed new correlation also includes surface tension, an important fluid property in small-channel flow boiling which is not found in the correlation of Lazarek and Black [26],but which was found

in the earlier correlation of Tran et al. [28] to help predict the R-113 and R-12 data well.

The new correlation is expected to be more representative, than either of these two earlier correlations of flow boiling in small channels, as attested to by the good agreement with the experimental data of three refrigerants over a range of pressures. The correlation is an improvement for the nucleate boiling term in the asymptotic model representing the heat transfer coefficient for flow boiling in small channels. It was also developed using experimental data from tests with three different refrigerants boiling at different pressures in circular and rectangular channels, with channel sizes in the range 2.4 to 2.9 mm. The correlation was represented by the following equations:

$$Nu = 770(\, Re_L \; N_{Conf} \; B_O \,)^{0.62} \left(\frac{\rho_V}{\rho_L}\right) \qquad \textit{(Eq. 23)}$$

$$N_{conf} = \frac{\left[\frac{\sigma}{g(\rho_L - \rho_V)}\right]^{0.5}}{d} \qquad \textit{(Eq. 24)}$$

$$B_O = \frac{q}{G \,.\Delta h_{vp}} \qquad \textit{(Eq. 25)}$$

$$h_{TP} = Nu \; \frac{K_L}{d} \qquad \textit{(Eq. 26)}$$

4.7 Other Correlations

More complex correlations have been developed by Shah [29], Steiner and Taborek [5], and Kattan et al.[30]. The Shah correlation appears to be no more reliable than the simpler methods given above. The Steiner-Taborek [5]correlation takes the form of the following general equation:

$$h_{tp} = [(a.\, h_{nb})^m + \left(b.\, h_{fc}\right)^m]^{1/m} \qquad \textit{(Eq. 27)}$$

where a = b =1 and m = 3. It was developed using a database containing over 13,000 data points for water, three alcohols, four hydrocarbons, four refrigerants, ammonia, nitrogen, and helium. All data are for convective boiling in vertical tubes. Although this method is among the best currently available in the open literature, the overall computational procedure is rather complicated and to some extent fluid specific.The correlation of Kattan et al. [30] is based on data for five refrigerants flowing in horizontal tubes, and is restricted to vapor fractions above 0.15 is used with a = b =1 and m = 3 , and the Cooper correlation[23] is used to calculate the nucleate boiling coefficient.

Different models are used to calculate the heat-transfer coefficient in each of four flow regimes: annular, stratified, stratified-wavy, and annular flow with partial dryout at high vapor fractions. All convective boiling correlations are developed and tested with experimental data for pure components, or in some cases, binary mixtures. Even for pure component boiling, they are not highly reliable when applied beyond the range of data used in their development. For the complex, often very non-ideal mixtures encountered in chemical and petroleum processing, their performance is still more problematic. Therefore, a relatively conservative approach to design, such as the use of Palen's method[31] for nucleate boiling of mixtures in conjunction with Chen's method, seems warranted. Note, however, that while this procedure will provide a conservative estimate for the nucleate boiling coefficient, the end result may not be conservative if the convective contribution or the suppression factor is overestimated by Chen's method. For pure components, and refrigerants in particular, the Liu–Winterton correlation is likely to be more reliable than the Chen correlation.

The correlations represented in the following Table 4 has been widely used for calculating the two-phase flow boiling heat transfer coefficient for different working fluids. Mainly, correlations are derived and tested with the experimental data for pure components and for binary mixtures at some instance.

Table 4 Flow boiling heat transfer correlations used in comparison

Reference	Correlation	Applicability range
Kew and Cornwell [32]	$h_{tp} = 30\ Re_L^{0.857}\ B_O^{0.714}\ \frac{K_L}{d}\ (1- x)^{-0.143}$	R141b d = 1.39 – 3.69 mm
Chaddock and Brunemann [33]	$h_{tp} = 1.91\ [\ (B_O \times 10^4) + 1.5(X_{tt}^{-1})^{0.67})]^{0.6}\ h_L$	
Lavin and Young [34]	$h_{tp} = 6.59\ h_L\ (\frac{1+x}{1-x})^{1.16}\ B_O^{0.1}$ $B_O = \frac{q}{G\ hfg}$	
Wojtan et al. [35]	$h_{tp} = S\ h_{sp}$ $h_{sp} = 55\ (P_r)^{0.12}\ (-\log P_r)^{-0.55}\ M^{-0.55}\ q^{0.67}$ S = 0.8	R-22 d= 13.84 mm
Oh and Son [36]	$h_{tp} = 0.03\ Re_f^{0.8}\ P_r^{0.3}\ [\ 1.58\ (X_{tt}^{-1})^{0.87}]\ \frac{K_f}{d}$	R-134a, R22 d= 1.77-5.35 mm
Pujol and Stenning [37]	$h_{tp} = 4\ (X_{tt}^{-1})^{0.87}\ h_L$	
Sun and Mishima[38]	$h_{tp} = [6\ Re_L^{1.05}\ B_O^{0.54}]\ [We_L^{0.191}\ (\rho_L/\rho_V)^{0.142}]^{-1}\ \frac{K_f}{d}$	R-410A
Hu et al. [39]	$h_{tp} = S\ h_{sp} + F\ h_L$ $F = 1+ 23969.60\ B_O^{1.16} + 1.294\ (X_{tt}^{-1})^{0.86}$ $S = (1+2.03x10^{-6}\ F^{1.58}\ Re_L^{1.17})^{-1}$ $h_{sp} = 55\ (P_r)^{0.12}\ (-\log P_r)^{-0.55}\ M^{-0.55}\ q^{0.67}$	

Each correlation has its own range of data, specific experimental geometry, type of channels (e.g., Macro, Mini channels) and type of fluid used in its development, in which going beyond it will not be highly reliable. Therefore, the data from various sources which could not be satisfactorily correlated by existing correlations were shown to be quite well correlated by their own data and the fluids that have been used in deriving their own correlations.

4.8 Proposed Developed Correlation

Flow boiling mainly depends on two main contributions which are the nucleate boiling and convective boiling. Therefore, achieving the balance between them is the key for better prediction as mentioned before by Chen[18]. Liu-Winterton correlation which show the highest accuracy for predicting the flow boiling heat transfer coefficient for pure ethanol stated in his correlation that it's not suitable to use the simple addition between the two contributions.

As the detailed comparison made by Gungor-winterton [22] showing that the heat transfer coefficient is considerably overpredicted in the high-quality region and underpredicted in the low-quality region. This indicates that the combination of the two heat transfer mechanisms by a simple addition method which is not very suitable.

Since in the high-quality region, even with a relatively small mass flow rate, the actual velocities of the phases must be extremely high and a great convective heat transfer intensity must be expected, hence the nucleate boiling mechanism must have been more greatly suppressed than that predicted by the Chen correlation[18].

Therefore, Kutateladze method [25] has been used to combine between the two contributions as follow:

$$h_{TP}^2 = [(S_{LW} . h_{nb})^2 + (E_{LW} . h_L)^2] \quad \textit{(Eq. 28)}$$

The correlations that have been evaluated with the available experimental data for pure ethanol shows only three correlation that shows an acceptable error band compared to the other correlations. The reason behind that is the data from various sources which could not be satisfactorily correlated by existing correlations were shown to be quite well correlated by their own data and the fluids that have been used in deriving their own correlations.

The generation of vapor itself in the boiling process results in significant disturbance of the layer and improved heat transfer. A dimensionless measure of how important this effect may be is given by the boiling number

$$B_o = \frac{q}{\Delta h_{vp} . G} \quad \textit{(Eq. 29)}$$

Boiling number is a dimensionless group representing a ratio between the mass of vapor generated at the heat transfer surface and mass flow rate per flow cross sectional area.

Since it was clearly demonstrated that the nucleate boiling contribution is dominant in predicting the boiling heat transfer coefficient. A new proposed suppression factor multiplier (Ms) is introduced to control the role of the nucleate boiling contribution either in over predicting or under predicting based on the regions correlated with boiling number (B_O) shown in Table 5.

The new suppression factor multiplier (Ms) is categorizing the over predicting and underpredicting regions in the dataset. As well as specific intervals are defined to control the over and under prediction in a precise way based on its's boiling number (B_O) interval based on the dataset analysis.

$$S = (1 + 1.15 \times 10^{-6} . E_{GW} . Re_L^{1.17})^{-1} \times Ms \qquad \textit{(Eq. 30)}$$

It has been observed that the nucleate boiling heat transfer contribution calculated from the pool boiling correlation of Cooper, should be reduced by 30% in region A for the specified interval mentioned in the Table 5.

The fact is, by increasing heat flux, cooper's method systematically overpredicts the measured heat transfer coefficient. As the deviation increases with increasing heat flux, it can be concluded that the nucleate boiling contribution is high. At this point, the role of the suppression factor multiplier shows up to achieve the balance between convective and nucleate boiling contributions by enhancing the suppression to the nucleate boiling to reduce its value.

On the other hand, the nucleate boiling heat transfer contribution calculated from the pool boiling correlation of Cooper tends to need enhancement to overcome the underprediction and to achieve a good balance between the nucleate and convective contributions for better results.

Therefore, the suppression factor multiplier (M_S) will function as a booster. The nucleate boiling should be increased by 10 ~ 50 % based the interval of the boiling number mentioned in the Table 5. These percentages are derived based on the analysis of the curves generated from the pure ethanol.

Table 5 Suppression factor multiplier values in each specified region

Region	Boiling number interval	M_s
A	$1\times 10^{-5} \leq BO < 1 \times 10^{-3}$	0.7
B	$1 \times 10^{-3} \leq BO < 5 \times 10^{-3}$	1.5
C	$5 \times 10^{-3} \leq BO < 1\times 10^{-2}$	1.3
D	$BO > 1 \times 10^{-2}$	1.1

4.9 Final Form of the Proposed Correlation

After the development applied to Liu-Winterton correlation, the new proposed development model predicts the experimental points more accurately specifically for pure ethanol. By using all the saturated boiling dataset for pure ethanol, the final form to calculate S and E and finally the final form for the correlation is as follow:

$$S = [(1 + 0.055 \,.\, E^{0.1} \,.\, Re_L^{0.16})^{-1} \times M_S] \qquad \textit{(Eq. 31)}$$

$$E_{LW} = [1 + x \,.\, P_{r_L} \frac{(\rho_L - \rho_V)}{\rho_V}]^{0.35} \qquad \textit{(Eq. 32)}$$

To be substituted in the following general equation:

$$h_{TP} = [(S \,.\, h_{nb})^2 \; + \; (E.h_L)^2]^{\frac{1}{2}} \qquad \textit{(Eq. 33)}$$

CHAPTER 5
Results and Discussion

The current experimental dataset included in the assessment consists of 722 flow boiling heat transfer coefficient data point for pure ethanol [4-7]. Therefore, the dataset of the experimental data is compared to the heat transfer coefficient correlations, to identify and discuss the most precise correlations in predicting those experimental values. The experimental conditions such as mass flux, heat flux, saturation temperature and vapor quality have been selected flux, saturation temperature and vapor quality have been selected based on the experimental data as shown in Table 6.

Table 6. Experimental conditions used in pure ethanol and ethanol/water mixture dataset

Parameters	**Range**
Saturation Temperature T_{sat} [°C]	40 – 86.6
Mass Flux G [kg/m^2 s]	0.33 – 290
Heat Flux q [Kw/m^2]	2.8 - 104
Internal Diameter d_{in} [mm]	5 - 10
Vapor Quality x	0.11 – 0.91

5.1 Assessment of previous correlations

Fourteen flow boiling heat transfer correlations were used for comparison with the experimental dataset. The correlations have been evaluated according to the mean absolute error (MAE); these data are presented in Table 6 for pure ethanol.

$$ER = \frac{h_{pred} - h_{exp}}{h_{exp}} \times 100 \qquad \textit{(Eq. 34)}$$

$$MAE = \frac{1}{N}\sum |ER| \qquad \textit{(Eq. 35)}$$

N: is the number of data points in dataset.

5.2 Analysis of pure ethanol

Flow boiling of pure component is not complicated compared to the corresponding binary mixtures. As its very smooth to find the thermo-physical properties at certain pressure and temperature. In addition, Heat transfer coefficient in pure component is mostly higher than the binary mixture at any concentrations as mentioned by Sarafraz et al.[40]. Tsutsui et al.[41] explained that heat transfer coefficient in pure component is usually higher in the low-quality region where the nucleate boiling is dominant. However, in the high-quality region the convective evaporative is dominant.

Peyghambarzadeh et al. [7] experimentally studied the effect of the working fluid among water, ethanol, and methanol on the thermal performance of a 40 cm circular copper heat pipe. The authors found that the use of ethanol led to higher heat transfer coefficient.

Mastrullo et al. [4] studied experimentally Anhydrous ethanol (purity grade of 99.8%) show a pure convective behavior, having an increasing trend with vapor quality up to the occurrence of dry-out.

Robertson et al. [5] experimentally investigated the vertical boiling of ethanol in 10 mm tube inside diameter, 3 m long was used in the experiment. The authors show

the interaction between nucleate and convective boiling as a function of vapor quality. Based on precise measurements of ethanol at saturation conditions. By analyzing the experimental dataset values and theoretical dataset which is the predicted values calculated by the mentioned flow boiling heat transfer correlations for pure ethanol has been made and the mean absolute error was calculated for each correlation as shown in Table 7.

Table 7 Prediction ability of the selected correlations with regard to the experimental dataset of Pure Ethanol.

Correlation	**MAE (%)**
Liu and Winterton [24]	25.79
Gungor and Winterton [22]	53.20
Kandlikar [27]	51.88
Lazarek and Black [26]	85.41
Chaddock and Brunemann [33]	77.08
Pujol and Stenning [37]	74.11
Chen [18]	28.28
Lavin and Young [34]	76.77
Tran et al. [28]	83.89
Kew and Cornwell [32]	83.95
Wojtan et al. [35]	40.11
Sun and Mishima [38]	29.89
Oh and Son [36]	66.06
Hu et al. [39]	57.83
Proposed correlation	15.5

Furthermore, figure 9 [A – F] shows a graphical representation of the performance of the polynomial curves for the aforementioned correlations. It is very

obvious that Liu-Winterton [24] Chen [18], Sun and Mishima [38]correlations have achieved the lowest MAE 25.05%, 28.28 % , 29.89 % respectively for the pure component of ethanol in various ranges of experimental conditions.

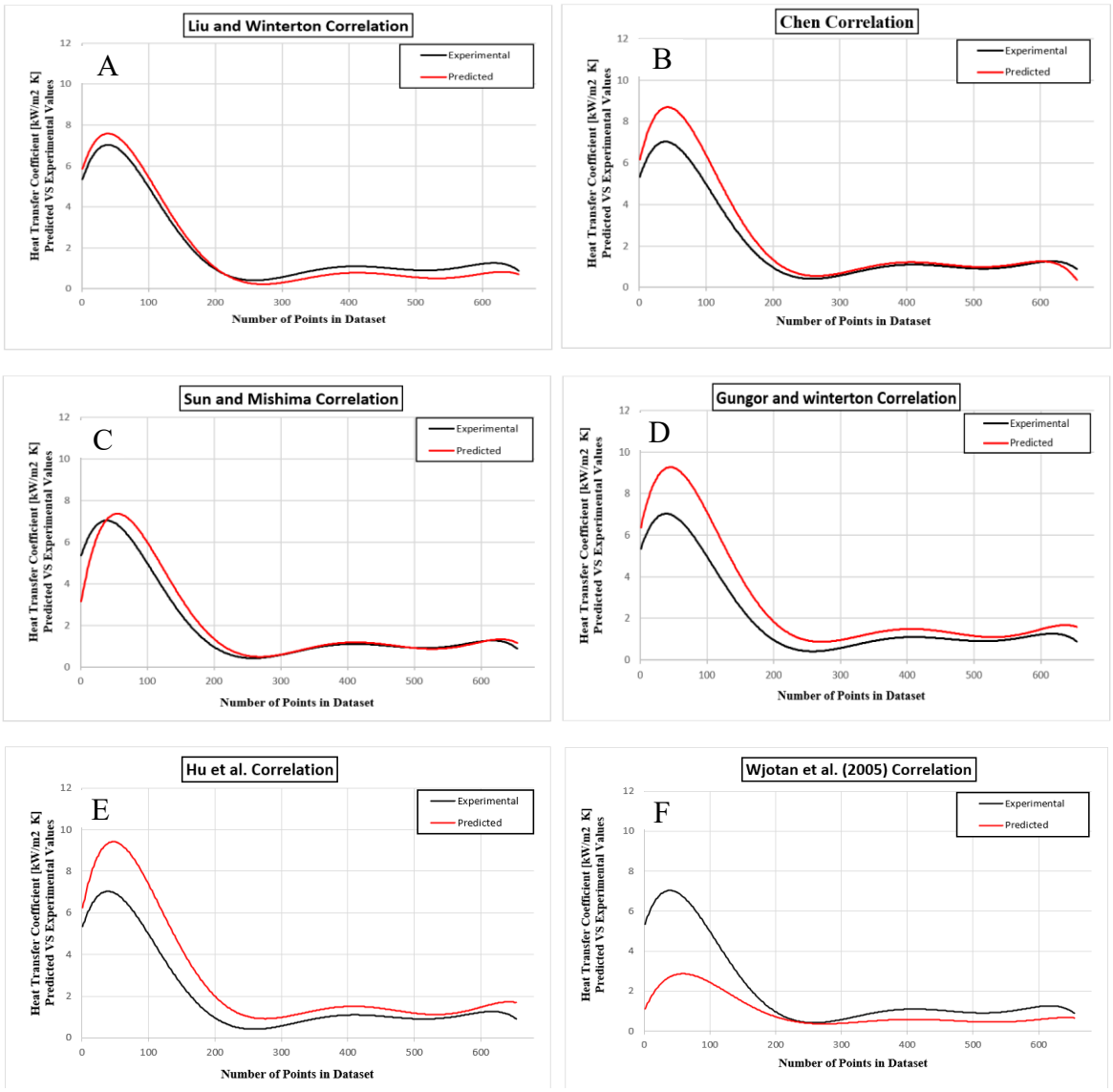

Figure 9 comparison between experimental values and the predicted values of the mentioned correlations

Also, the scatter plots in Figure 10,11,12 shows the performance of the top three correlation within an error band of ±30 %.

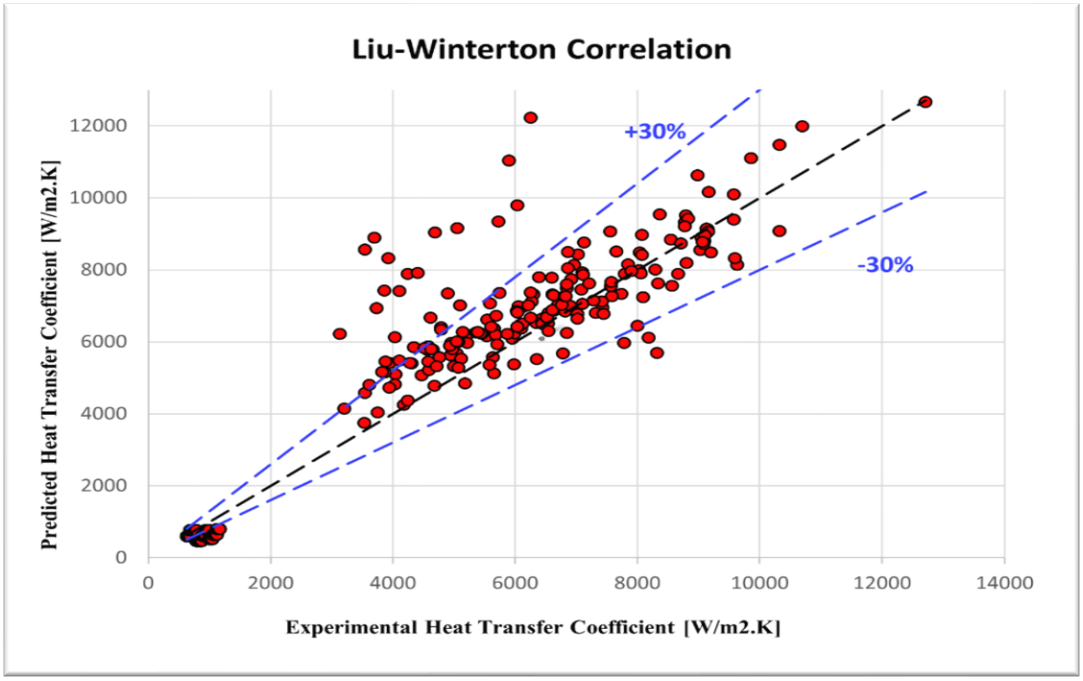

Figure 10 Experimental Values versus Predicted Values for Liu-Winterton Correlation within a band error ±30 %

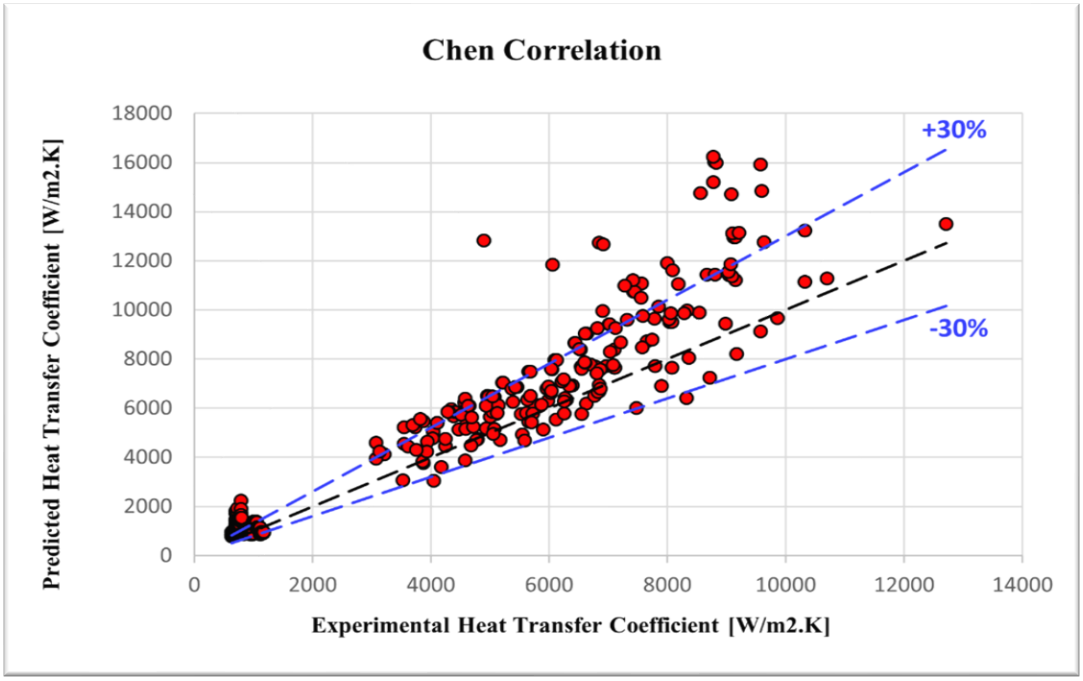

Figure 11 Experimental Values versus Predicted Values for Chen Correlation within a band error ±30 %

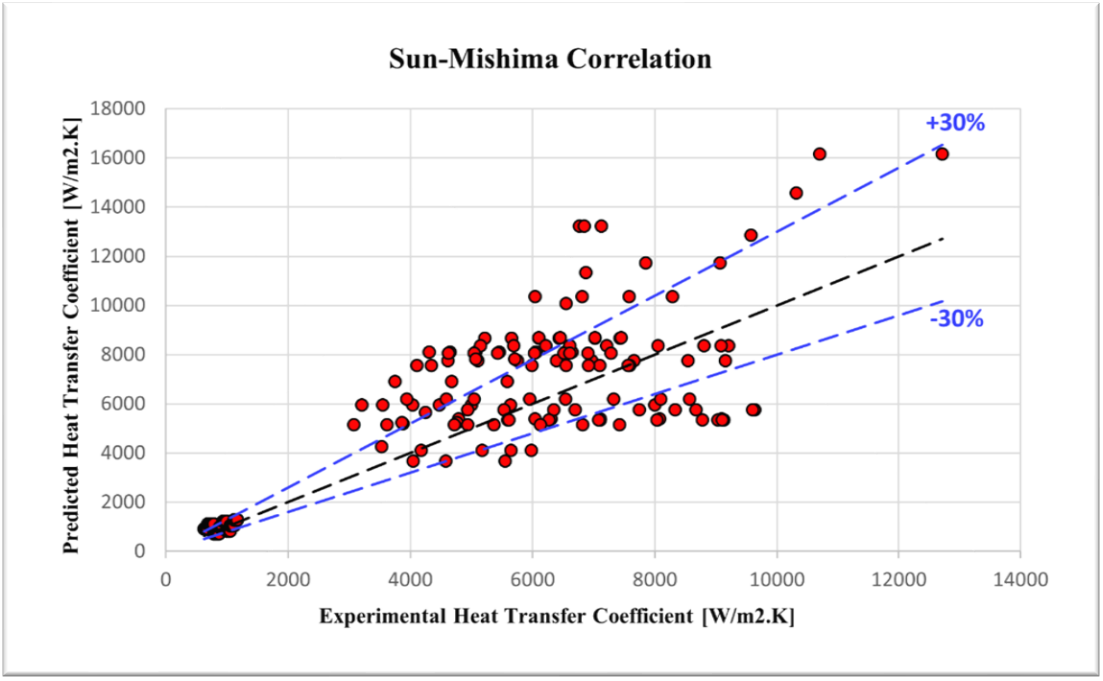

Figure 12 Experimental Values versus Predicted Values for Sun-Mishima Correlation within a band error ±30 %

5.3 Comparison between correlations

It was mentioned earlier in the results that Liu-Winterton [24] Chen [18], Sun and Mishima [38]correlations have achieved the lowest MAE 25.05%, 28.28 % , 29.89 % respectively for the pure component of ethanol in various ranges of experimental conditions. The new proposed correlation has proved a good standing accuracy by achieving an error margin of 15.5% as shown in Figure 13.

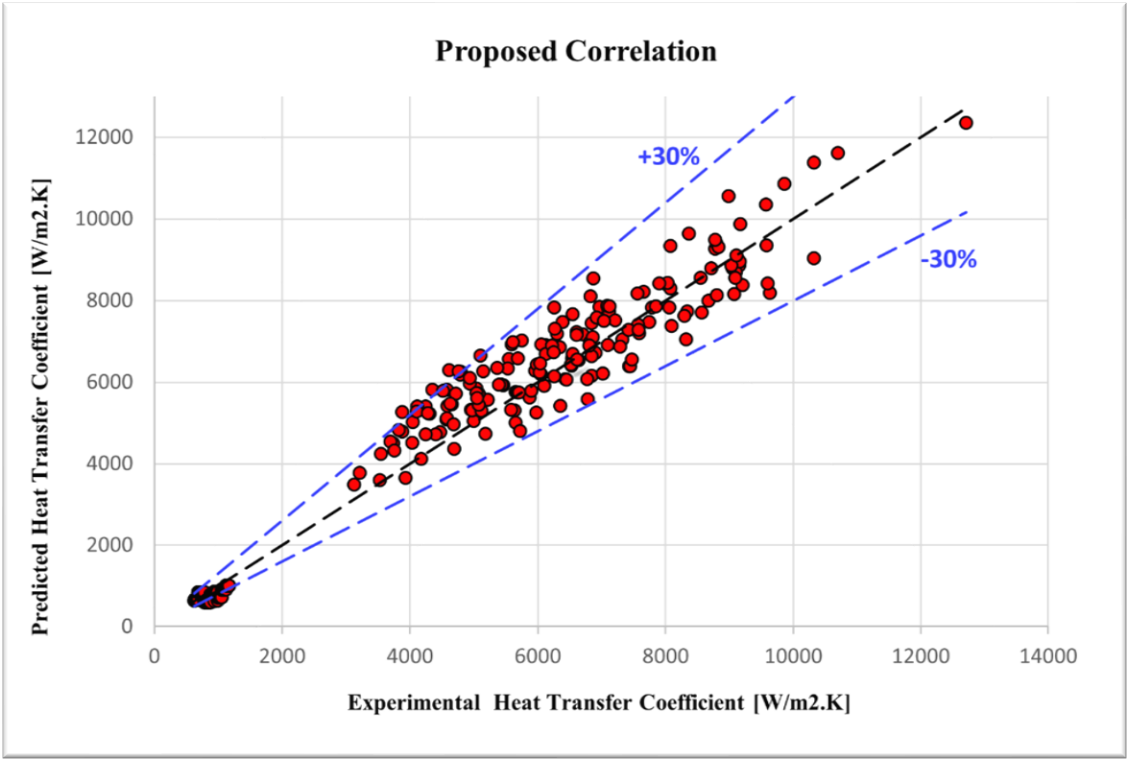

Figure 13 Experimental Values versus Predicted Values for New Proposed Correlation within a band error ±30 %

Liu-Winterton correlation which is considered to be the best correlation among the 14 correlation that have been used in such as study achieved the lowest band error which is reduced from 25.05 % into 15.5%. Therefore, the proposed correlation has succeeded to reduce the best fit correlation by 9.6% as shown in Figure 14,15.

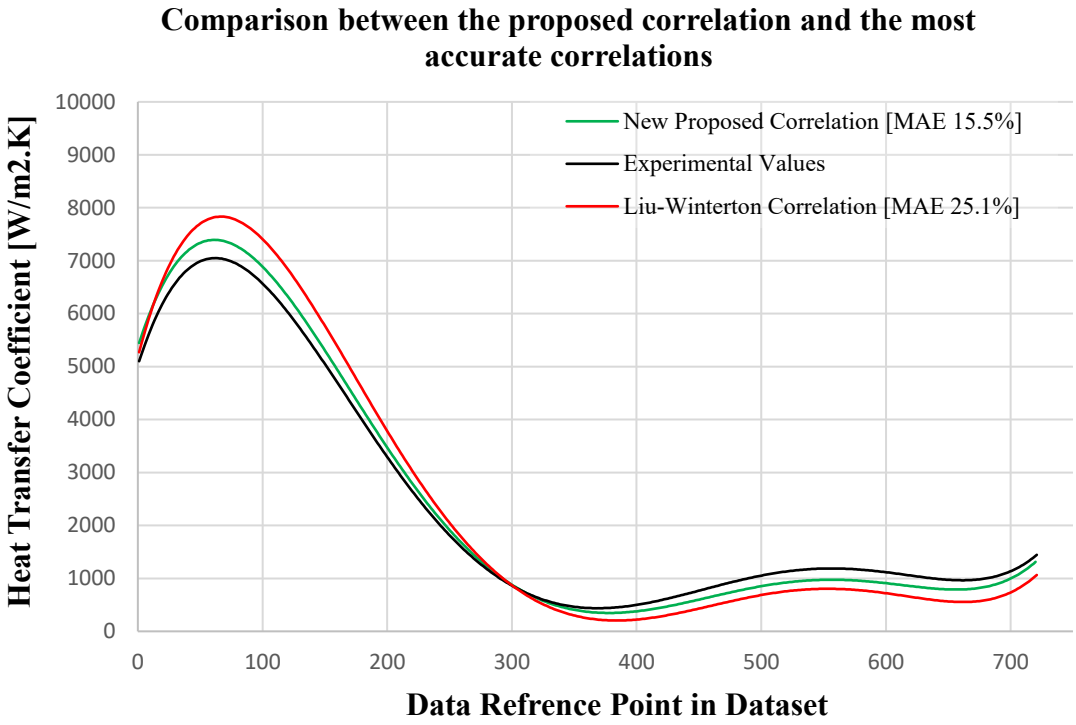

Figure 14 Comparison between the proposed correlation and the most accurate correlation.

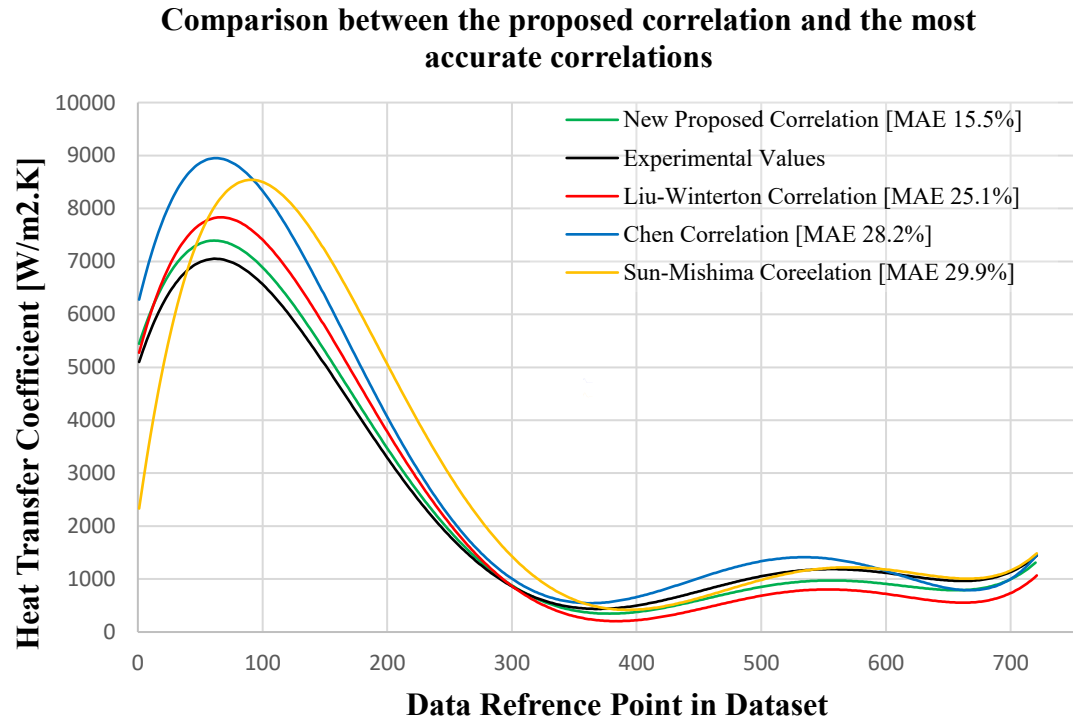

Figure 15 Comparison between the proposed correlation and the most accurate correlations

CHAPTER 6
Conclusion and Future Works

6.1 CONCLUSIONS

After comparing the experimental dataset included in the assessment which consists of 720 flow boiling heat transfer coefficient data point for pure ethanol with some of the available correlations in literature:

1- It is very clear that Liu-Winterton [24],Chen [18] and Sun and Mishima [38] correlations are precise in prediction compared to the rest.
2- A new proposed correlation has been developed by introducing a suppression factor multiplier (M_S).
3- The proposed correlation has succeeded to reduce the error band by 9.5% compared to Liu-Winterton correlation.

Finally, most of the correlations are derived and tested with the experimental data for pure components. Each correlation has its own range of data, specific experimental geometry, type of channels (e.g., Macro, Mini channels) and type of fluid used in its development, in which going beyond it will not be highly reliable. Therefore, the data from various sources which could not be satisfactorily correlated by existing correlations were shown to be quite well correlated by their own data and the fluids that have been used in deriving their own correlations.

6.2 FUTURE STUDIES

A huge shortage in the experimental data concerning pure ethanol in literature. Therefore, more experimental work should be done for pure ethanol as it's a very promising fluid in many industrial applications. Furthermore, it's recommended to use the range of heat flux from 7 kW/m^2 ~ 20 kW/m^2 to fill the gap shown in Figure [10~14] which almost from 1 kW/m^2 K to 3 kW/m^2 K in each Figure. Moreover, Testing the new proposed correlation with other pure fluids and binary mixtures to check its efficiency.

References

[1] L.S. Tong, Y.S. Tang, Boiling heat transfer and two-phase flow, Routledge, 2018.

[2] t.E. Heat and Mass Transfer - Fundamentals and Applications, McGraw-Hill Education, New York, NY, 2020.

[3] R.W. Serth, T. Lestina, Process heat transfer: Principles, applications and rules of thumb, Academic press, 2014.

[4] R. Mastrullo, A. Mauro, R. Revellin, L. Viscito, Flow boiling heat transfer and pressure drop of pure ethanol (99.8%) in a horizontal stainless steel tube at low reduced pressures, Publisher, City, 2018.

[5] D. Steiner, J. Taborek, Flow boiling heat transfer in vertical tubes correlated by an asymptotic model, Publisher, City, 1992.

[6] P. Vasileiadou, K. Sefiane, T.G. Karayiannis, J.R. Christy, Flow boiling of ethanol/water binary mixture in a square mini-channel, Publisher, City, 2017.

[7] S. Peyghambarzadeh, S. Shahpouri, N. Aslanzadeh, M. Rahimnejad, Thermal performance of different working fluids in a dual diameter circular heat pipe, Publisher, City, 2013.

[8] M.C. Diaz, J. Schmidt, Experimental investigation of transient boiling heat transfer in microchannels, Publisher, City, 2007.

[9] I. Mudawar, Assessment of high-heat-flux thermal management schemes, Publisher, City, 2001.

[10] W. Li, Z. Wu, A general criterion for evaporative heat transfer in micro/mini-channels, Publisher, City, 2010.

[11] G. Hewitt, A. Govan, Phenomenological modelling of non-equilibrium flows with phase change, Publisher, City, 1990.

[12] R. Nedderman, Boiling, Condensation Gas-Liquid Flows. By PB Whalley. Oxford Science Publication, 1987. 291 pp.£ 40, Publisher, City, 1988.

[13] A. Dukler, Y. Taitel, Flow pattern transitions in gas-liquid systems: measurement and modeling, Publisher, City, 1986.

[14] A. Biesheuvel, W. Gorissen, Void fraction disturbances in a uniform bubbly fluid, Publisher, City, 1990.

[15] A. Govan, G. Hewitt, H. Richter, A. Scott, Flooding and churn flow in vertical pipes, Publisher, City, 1991.

[16] N. Shiro, The maximum and minimum values of the heat Q transmitted from metal to boiling water under atmospheric pressure, Publisher, City, 1984.

[17] J. Xu, Y. Wang, R. Yang, W. Liu, H. Wu, Y. Ding, Y. Li, A review of boiling heat transfer characteristics in binary mixtures, Publisher, City, 2021.

[18] J.C. Chen, Correlation for boiling heat transfer to saturated fluids in convective flow, Publisher, City, 1966.

[19] W. Zhang, T. Hibiki, K. Mishima, Correlation for flow boiling heat transfer in mini-channels, Publisher, City, 2004.

[20] W. Chen, X. Fang, A note on the Chen correlation of saturated flow boiling heat transfer, Publisher, City, 2014.

[21] H. Forster, N. Zuber, Dynamics of vapor bubbles and boiling heat transfer, Publisher, City, 1955.

[22] K.E. Gungor, R. Winterton, A general correlation for flow boiling in tubes and annuli, Publisher, City, 1986.

[23] M. Cooper, Heat flow rates in saturated nucleate pool boiling-a wide-ranging examination using reduced properties, in: Advances in heat transfer, Elsevier, 1984, pp. 157-239.

[24] Z. Liu, R. Winterton, A general correlation for saturated and subcooled flow boiling in tubes and annuli, based on a nucleate pool boiling equation, Publisher, City, 1991.

[25] S.S. Kutateladze, Boiling heat transfer, Publisher, City, 1961.

[26] G. Lazarek, S. Black, Evaporative heat transfer, pressure drop and critical heat flux in a small vertical tube with R-113, Publisher, City, 1982.

[27] S.G. Kandlikar, A general correlation for saturated two-phase flow boiling heat transfer inside horizontal and vertical tubes, Publisher, City, 1990.

[28] T. Tran, M. Wambsganss, D. France, Small circular-and rectangular-channel boiling with two refrigerants, Publisher, City, 1996.

[29] M.M. Shah, Chart correlation for saturated boiling heat transfer: equations and further study, Publisher, City, 1982.

[30] N. Kattan, J.R. Thome, D. Favrat, Flow boiling in horizontal tubes: part 3—development of a new heat transfer model based on flow pattern, Publisher, City, 1998.

[31] J. Palen, J. Taborek, S. Yilmaz, Comments to the application of enhanced boiling surfaces in tube bundles, in: Advanced Course in Heat Exchangers: Theory and Practice. ICHMT Symposium., Begel House Inc., 1981.

[32] P.A. Kew, K. Cornwell, Correlations for the prediction of boiling heat transfer in small-diameter channels, Publisher, City, 1997.

[33] J.B. Chaddock, and Brunemann, H., Forced Convection Boiling of Refrigerants in Horizontal Tubes: Phase 3, Laboratories., in, Duke University, Durham., 1967.

[34] J.G. Lavin, E.H. Young, Heat transfer to evaporating refrigerants in two-phase flow, Publisher, City, 1965.

[35] L.U. Wojtan, Thierry & Thome, John. , Investigation of Flow Boiling in Horizontal Tubes: Part II, Development of a New Heat Transfer Model for Stratified-Wavy, Dryout and Mist Flow Regimes., Publisher, City, 2004.

[36] H.-K. Oh, C.-H. Son, Evaporation flow pattern and heat transfer of R-22 and R-134a in small diameter tubes, Publisher, City, 2011.

[37] L.P.a.A.H. Stenning., Effect of Flow Direction on the Boiling Heat Transfer Coefficient in Vertical Tubes, Proc . Int. Symp. Concurrent Gas-Liquid Flow, , in, Univ . of Waterloo, Canada, Sept. 1968, pp . 401-453 .

[38] L. Sun, K. Mishima, An evaluation of prediction methods for saturated flow boiling heat transfer in mini-channels, Publisher, City, 2009.

[39] H. Hu, G. Ding, X.-C. Huang, B. Deng, Y.-F. Gao, Experimental investigation and correlation of two-phase heat transfer of R410a/oil mixture flow boiling in a 5-mm microfin tube, Publisher, City, 2011.

[40] S.M.P. M.M. Sarafraz , N. Vaeli ,Subcooled Flow Boiling Heat Transfer of Ethanol Aqueous Solutions in Vertical Annulus Space, Chem. Ind. Chem Eng. Q. 18 (2) (2012) 315–327, Publisher, City.

[41] T.W.L. M. Tsutsui , Y. Fujita Heat Transfer and Pressure Drop in Flow Boil- ing of Binary Mixtures in a Uniformly Heated Horizontal Tube, in: Proceedings of the 4th JSME-KSME Thermal Engineering Conference, Kobe, Japan, Japan, 2000.

[42] Å. Melinder, Thermophysical Properties of Aqueous Solutions Used as Secondary Working Fluids., in: Energy Technology, Royal Institute of Technology, KTH, Stockholm, Sweden, 2007.

Appendix

The phase diagram for ethanol shows the phase behavior with changes in temperature and pressure.

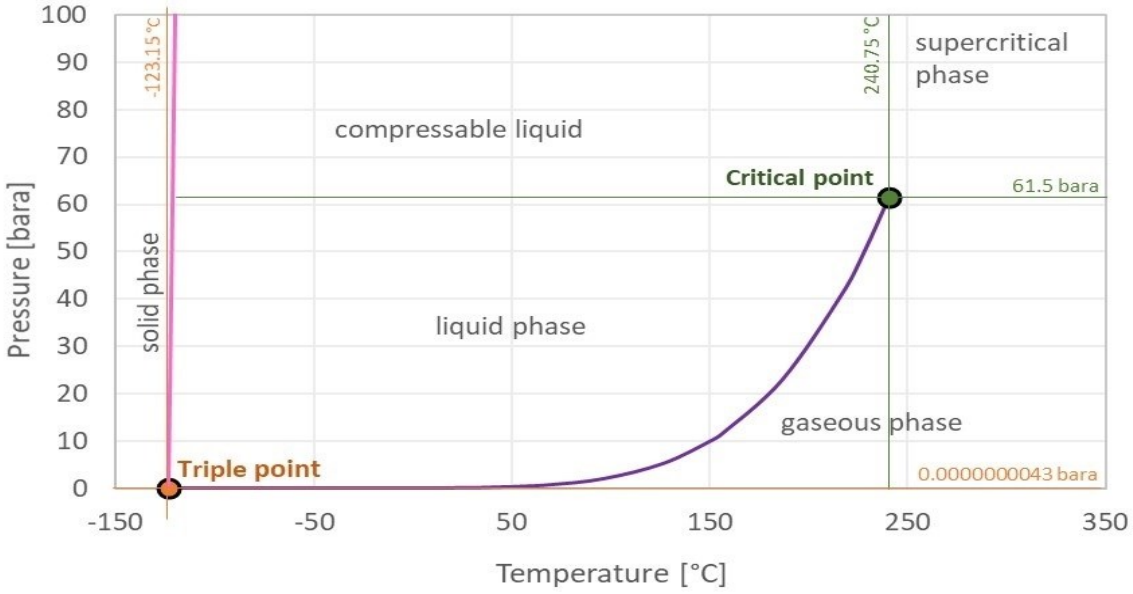

Figure 16 Ethanol Phase Diagram[42]

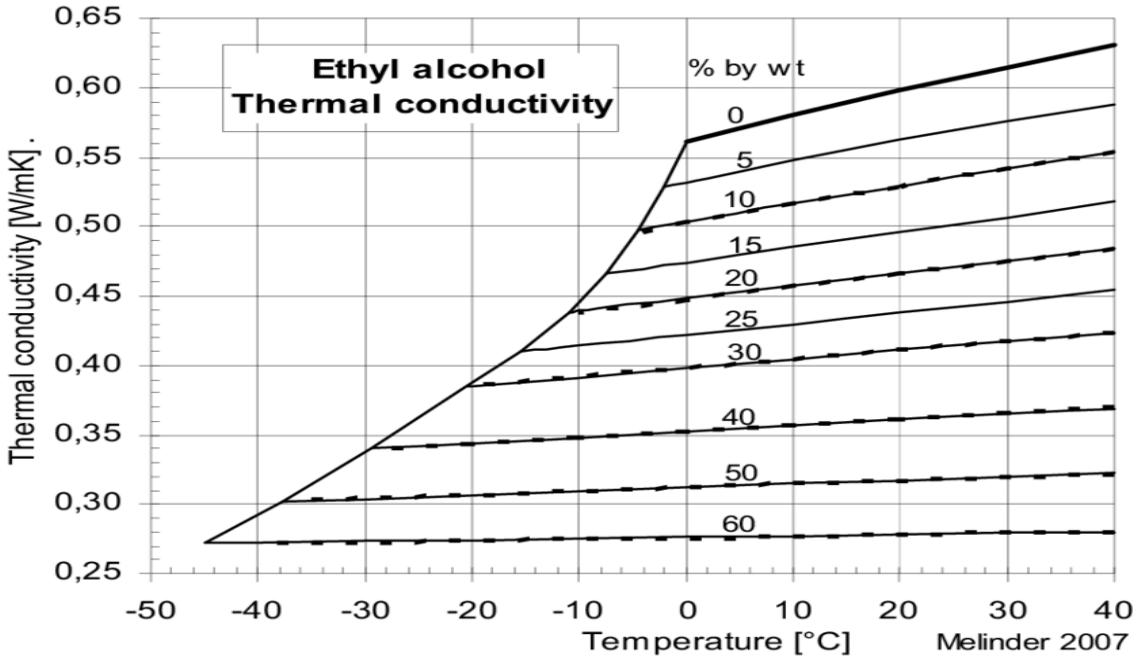

Figure 17 Ethanol Thermal Conductivity Curve[42]

Table 8 Basic Thermo-physical properties of ethanol [43]

t_F [°C]	c_A [wt-%]	t [°C]	ρ [kg/m³]	c_p [J/kgK]	k [W/mK]	μ [mPas]
0	0	40	992.2	4177	0.631	0.653
		30	995.7	4177	0.615	0.798
		20	998.2	4181	0.598	1.002
		10	999.7	4192	0.580	1.306
		0	999.9	4218	0.561	1.792
-2.09	5	40	983.1	4235	0.588	0.77
		30	986.6	4235	0.576	0.96
		20	989.5	4240	0.562	1.24
		10	990.8	4270	0.548	1.70
		0	991.4	4325	0.532	2.45
		-2.09	991.2	4340	0.528	2.70
-4.47	10	40	974.9	4270	0.554	0.90
		30	978.7	4270	0.542	1.16
		20	982.0	4280	0.529	1.53
		10	983.8	4310	0.516	2.17
		0	984.9	4360	0.503	3.25
		-4.47	985.1	4390	0.498	4.20
-7.36	15	40	966.8	4320	0.518	1.03
		30	971.2	4310	0.507	1.35
		20	975.2	4320	0.496	1.84
		10	978.0	4340	0.485	2.70
		0	979.9	4370	0.474	4.20
		-7.36	980.5	4410	0.466	6.5

Chemical formula: C_2H_5OH; M = 46.07